Available online at www.sciencedirect.com

ScienceDirect

Procedia Structural Integrity 37 (2022) 105–114

Structural Integrity Procedia

www.elsevier.com/locate/procedia

ICSI 2021 The 4th International Conference on Structural Integrity

A method for determining the distribution of carbon nanotubes in nanocomposites by electric conductivity

Dayou Ma[a,*], Ali Esmaeili[a], Claudio Sbarufatti[a], Marco Giglio[a], Andrea Manes[a]

[a]*Politecnico di Milano, Department of Mechanical Engineering, via la Masa, 1, 20156, Milan, Italy*

Abstract

Carbon nanotube (CNT) polymer nanocomposites are one of the most promising materials due to their remarkable mechanical properties as well as the electrical conductivity, which offers the capability of monitoring the deformation and damage of composite structures by measuring the related conductivity variations. However, quantifying the distribution of CNTs inside the material remains a challenge with respects to both experimental and numerical works. In the current study, the electrical conductivity was used to determine the microstructure of CNT-reinforced polymer. By introducing a modified parameter related to the polar angle of CNTs, the mechanical properties as well as the electrical conductivity change with respect to deformation of nanocomposites can be replicated. After validation by experimental data from the multi-walled CNT/polymer nanocomposites under tensile loading, the capability of the current method was then studied for composites with various weight fractions of nanotubes.

Keywords: mechanical properties; tensile loading; effective length; finite element model; analytical model

1. Introduction

Carbon nanotube (CNT) based nanocomposites are one of the most promising types of advanced materials resulted in enhancement of physical properties, such as electrical conductivity, improved strength but preserving low density. In addition, CNTs can make the nanocomposite conductive, which offers the capability of monitoring the deformation and damage of composite structures by measuring the relative resistance change. However, the choice of the correct amount of CNT (weight fractions), as well as their effects on electro-mechanical properties are not straightforward. An investigation based only on experimental tests may be not completely effective. The use of numerical methods may help in providing an insight both into the mechanical and electrical properties of this kind of material. Numerical

* Corresponding author. Tel.: +39 02 2399 8474.
E-mail address: Dayou.ma@polimi.it

10.1016/j.prostr.2022.01.065

models may provide a detailed understanding and analysis on the physical mechanism of nanocomposites (Liu and Chen 2003).

The electrical property of CNT-doped nanocomposites has been widely investigated due to the aforementioned potentials (Coleman et al. 1998). The mechanism for electric conductivity can be attributed to the tunnelling effect arisen from CNT networks (Danikas, n.d.): when CNTs are close enough inside the matrix, dielectric breakdown occurs through the matrix and the tunnel, where electrons pass. Therefore, the effective current path can be established to make the composite electrically conductive. Knowing mechanism of electrical conductivity, modelling such phenomena focused on the electrical property of nanocomposites has drawn great attention. Li et al. (Li, Thostenson, and Chou 2007) proposed a calculation method for electrical resistance of tunnelling effect. Coupled with the Landauer-Buttiker (L-B) model and the Monte-Carlo method, an electrical model was built with a high efficiency (Bao et al. 2012; Zabihi and Araghi 2016).

Molecular dynamics (MD) simulation and finite element (FE) method are the two main methods mainly used for mechanical properties simulation. The former is able to model the nanocomposites considering their molecular structures, which allows further investigation of the effect of CNTs on the mechanical properties (Frankland et al. 2003; Alian and Meguid 2017; Alian, El-Borgi, and Meguid 2016), but long calculation time and parameters of the chemical bond property hindered its application (Alian and Meguid 2017, 2018a). On the other hand, FE method is widely used on nanocomposites because of its reliability under various loading conditions for complicated structures on different scales (X. L. Chen and Liu 2004; Ma et al. 2021).

Furthermore, monitoring the deformation using piezoresistive properties of the CNT doped epoxy nanocomposites was investigated experimentally and analytically (Esmaeili, Sbarufatti, et al. 2020; Sánchez-Romate et al. 2018; Hu et al. 2008). Recently, it was reported that a previous analytical model can be enhanced so that the resistance of nanocomposites during loading can be replicated by combination with the FE method (Alian and Meguid 2018b; Khattab and Sinapius 2019), in view that the FE model can help to obtain accurate deformation of the nanocomposites and the orientation of CNT implanted inside composites. All these studies indicate that a numerical methodology can replicate the current path and predict the electrical properties of nanocomposites.

Among all these studies, however, some aspects about the modelling process have yet to be explored. Only one/few CNTs can be contained in the numerical model because of computational costs (Alian and Meguid 2017; Alian, El-Borgi, and Meguid 2016; Alian and Meguid 2018a), or random CNT generation was employed to build the CNT network inside nanocomposites (Bao et al. 2012, 2013, 2011; Alian and Meguid 2018b). On the other hand, the accurate structure of the nanocomposites cannot be modelled because nanoparticles inside the polymer materials are hard to detect experimentally without cutting the samples (Alian and Meguid 2018c; Hu et al. 2008). Besides, due to the loss of representation of the real micro-structure, the accuracy might be affected in the modelling process. Compared with the aligned-CNT-doped nanocomposites (Ma, Giglio, and Manes 2020b), modelling nanocomposites with non-aligned CNTs is more difficult considering the significant effect of the waviness of CNTs (Khan, Pothnis, and Kim 2013). Thanks to the simplified methodology for modelling of waved CNTs (X. Chen, Alian, and Meguid 2019; Shams and Soltani 2017), it paved the path for replicating the waved CNTs based on modelling strategies for aligned CNTs.

Therefore, the present study was aimed to explore the possibility of using the electrical property to build the mechanical model, as the scheme to present the methodology in Fig. 1. Firstly, an electrical model with the effective CNTs, which can help to model with aligned one numerically, was used to define the microstructure of the nanocomposite by the initial electrical conductivity, which could help to detect the inner CNT networks of nanocomposites for mechanical modelling. Then, the representative volume element (RVE) model was built in FE method based on the electrical model to study the mechanical property of the nanocomposite with high accuracy and efficiency, which can be validated by the experimental data. Furthermore, the electromechanical behaviour of the nanocomposite was replicated and assessed.

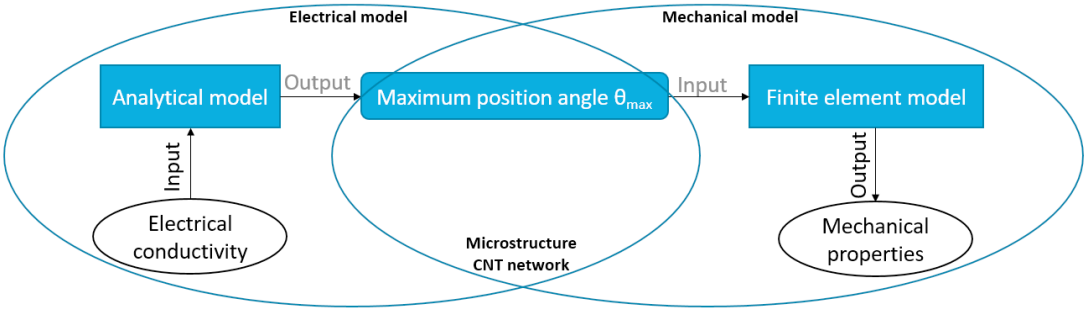

Fig. 1 Scheme for the current modelling strategy

2. Simulation procedure

2.1 Electrical model

Generally, CNTs in polymer materials are randomly distributed and waved without an aligning process. However, in order to simplify the modelling in the present study, the concept of effective CNT was introduced with start and end points of an actual CNT, as visible in Fig. 2. Therefore, in our modelling process, the actual CNT can be described by the effective CNT with a line segment. Considering random distribution of CNTs inside the matrix, the start point of CNT (x_i, y_i, z_i) is generated according to Eq.(1), where L_Θ is the length of the electrical representative volume element (RVE) of nanocomposite along different directions and RAND is a uniform random number in the interval [0,1].

$$\Theta_i = L_\Theta \times RAND \ (\Theta = x, y, z. i = 1,2, \dots) \tag{1}$$

For an effective CNT built as a line segment in Fig. 2, θ is polar angle defined by the maximum polar angle θ_{max} (Eq.(2)), while the azimuthal angle ϕ was generated inside [0, 2π] randomly (Eq.(3)). If $\theta_{max} = 0$, all effective CNTs are along one single direction; if $\theta_{max} = \pi/2$, the nanocomposite can be regarded as isotropic, which means the orientation of the effective CNT has no influence anymore because of the total random generation.

$$cos\theta = (1 - cos\theta_{max}) \times RAND + cos\theta_{max} \tag{2}$$

$$\phi = 2\pi \times RAND \tag{3}$$

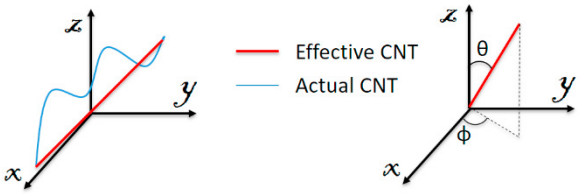

Fig. 2 Schematic diagram for CNT inside nanocomposite

As for the length of CNTs, an average length $\acute{l}$ was used and regarded as the effective length in the present study. According to (Wang et al. 2006), the length of CNTs follows a Weibull distribution, based on which the average length $\acute{l}$ can be calculated (Bao et al. 2011). Subsequently, the end point of ith CNT can be described as $(x_i + \acute{l}sin\theta_i cos\phi_i, y_i + \acute{l}sin\theta_i sin\phi_i, z_i + \acute{l}cos\theta_i)$. Moreover, if the end point is located outside of the electrical RVE, the CNT would be directly cut by the boundary. In this way, a random microstructure of nanocomposite can be built in electrical RVE.

The overall resistance of such CNT doped nanocomposite is composed of two individual types. One is the intrinsic resistance of CNT, R_{CNT}, and the other one is the contact resistance between two closest CNTs, $R_{contact}$. R_{CNT} can be obtained through Eq.(4), where σ_{CNT} is the intrinsic CNT electrical conductivity and the cross section of the CNT is

regarded as perfect circle, D is the diameter of the CNT. The contact resistance is provided by the tunnelling effect introduced. According to the L-B model (Büttiker et al. 1985), $R_{contact}$ is defined by Eq.(5), where M is the number of tunnelling channels, h is the Planck's contact and e is the electron charge, so $\frac{h}{2e^2} \approx 12.9054k\Omega$ is equal to the quantized resistance. Moreover, T is represented as the transmission probability to breakdown of the matrix between two CNTs, which is determined by Eq.(6) based on the Wentzel-Kramers-Brillouin (WKB) approximation (Simmons 1963). Regarding the Pauli exclusion principle (Hertel, Walkup, and Avouris 1998), the closest distance between two CNTs, d, should be larger than the van deer Waals separation distance, d_{vdW}. So, if d is smaller than d_{vdW}, it should be replaced by d_{vdW}. When d is greater than d_{vdW}, the real distance is equal to $(d - D)$ considering the diameter of the CNT. The tunneling effect can be ignored if the distance is larger than the cut-off distance, d_{cutoff}. Moreover, the tunnelling characteristic length is defined by $d_{tunnel} = \hbar/\sqrt{8m_e\Delta E}$, d_{tunnel}. In the definition of d_{tunnel}, ΔE is the height of the barrier between the polymer and CNT and m_e is the mass of the electron.

$$R_{CNT} = \frac{4\acute{l}}{\pi\sigma_{CNT}D^2} \tag{4}$$

$$R_{contact} = \frac{h}{2e^2}\frac{1}{MT} \tag{5}$$

$$T = \begin{cases} exp\left(\frac{-d_{vdW}}{d_{tunnel}}\right), 0 \le d \le D + d_{vdW} \\ exp\left(\frac{-d-D}{d_{tunnel}}\right), D + d_{vdW} \le d \le D + d_{cutoff} \end{cases} \tag{6}$$

In the present study, the distance between two CNTs was calculated through the methodology mentioned in (Eberly 2001). Following the calculation, a matrix of the distance can be obtained. Then, the matrix of all potential resistances can be calculated by Eq. (5,6). Subsequently, a search algorithm was employed to obtain the effective current method in the CNT system, as shown in Fig. 3 in which all the effective current paths are in parallel. Additionally, a Monte-Carlo simulation with a 10000-time calculation was used to simulate this electrical model in multiple cases, while MATLAB was employed to perform the abovementioned process.

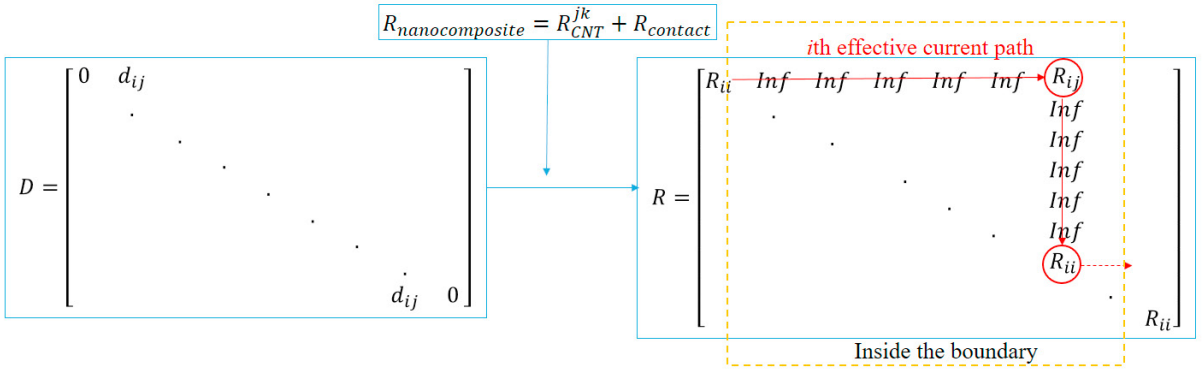

Fig. 3 Numerical method for the resistance of electrical RVE

In order to validate the electrical model, a calculation case was used. In this case, MWCNT was implanted into the polymer, and all the data used in the present model were obtained by Ref. (Bao et al. 2011): $\sigma_{CNT} = 5 \times 10^3$S/m, $\Delta E = 1$ eV, $\acute{l} = 5$ μm, $D = 50$ nm, $M = 460$, $L_x = L_y = L_z = 5.5$ μm, $\theta_{max} = \frac{\pi}{2}$, $d_{vdW} = 3.4$ Å and $d_{cutoff} =$ 1.4nm. The change in conductivity with the volume fraction is shown in Fig. 4. In Fig. 4, the results obtained through the present model correspond with the experimental data. As the volume fraction increases, the growing trend of the electrical conductivity is initially sharp and then becomes gentle. This can be attributed to percolation threshold region, the region that the tunnelling effect plays the domain role in generating the effective current. In other words, at low CNTs content, electrical conductivity sharply increase with respect to CNT content. On the contrary, at high CNT loading i.e. above percolation threshold region, the growth of electrical conductivity is less tangible due to the

saturation point of the tunnelling effect, which is the percolation threshold. In this case, the percolation threshold is around 0.75 vol.% according to the present electrical model, which has good agreement with the results from Ref(Hu et al. 2008; Bao et al. 2011). The present electrical model has therefore been validated through comparison with experimental data and has demonstrated its capability to be used in the next stage. In the present study, the electrical model introduced in this section was used to obtain the maximum polar angle θ_{max}.

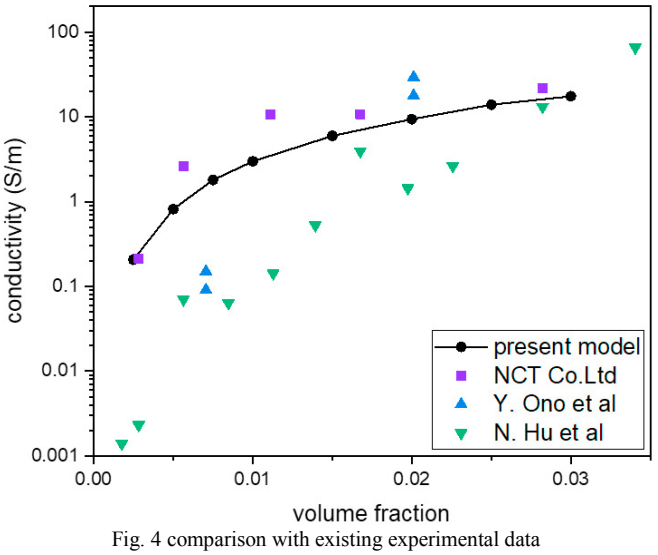

Fig. 4 comparison with existing experimental data

2.2 Mechanical model

Through the initial electrical conductivity, the structure of the nanocomposite can be determined to study its mechanical property. As mentioned in the Section 1, the mechanical properties are hard to model in FEM as the size gap between CNT and RVE hinders the generation of the mesh. In the present study, the mechanical RVE model was one of several parts selected from the electrical model, which was built in Section 2.1, as shown in Fig. 5. As a result, the mechanical model can be simplified instead of using the large-scale electrical RVE model. Every part, containing more than two CNTs, should be selected and built in the FE framework separately. Therefore, there should be more than one mechanical models in one case, while the exact number of mechanical models is determined by the electrical properties. More details of the modelling procedure can be found in Fig. 5, and the FE model was built in LS-DYNA.

In order to simplify the geometry and make the contact smooth, voxel mesh was used to mesh the mirco-RVE model, as applied in previous work (Ma, Manes, and Giglio 2019; Ma, Giglio, and Manes 2020a, 2020b). The contact between CNT and matrix was described by a tiebreak contact algorithm in LS-DYNA. The loading was uniaxial tension in the direction along x-, y- and z-axial namely, and the load was applied by displacement control. It should be noted that the size of the mechanical RVE models in one case should be identical in order to assist the simplification of the post calculation of the mechanical properties. Based on this simplification, all the mechanical RVEs share the same strain along the loading direction. As a result, Eq. (7) is used to calculate the real mechanical properties of nanocomposite. In Eq.(7), n is the number of mechanical RVE models, A^{Θ} is the area of the cross section with the normal of Θ, while ε and σ represent the strain and stress namely.

$$\begin{cases} \varepsilon^{\Theta} = \varepsilon_1^{\Theta} = \cdots = \varepsilon_n^{\Theta} \\ \sigma^{\Theta} = [\sum_{i=1}^{n} \sigma_i^{\Theta} \cdot A_i^{\Theta}]/(\sum_{i=1}^{n} A_i^{\Theta}) \end{cases}, (\Theta = x, y, z) \tag{7}$$

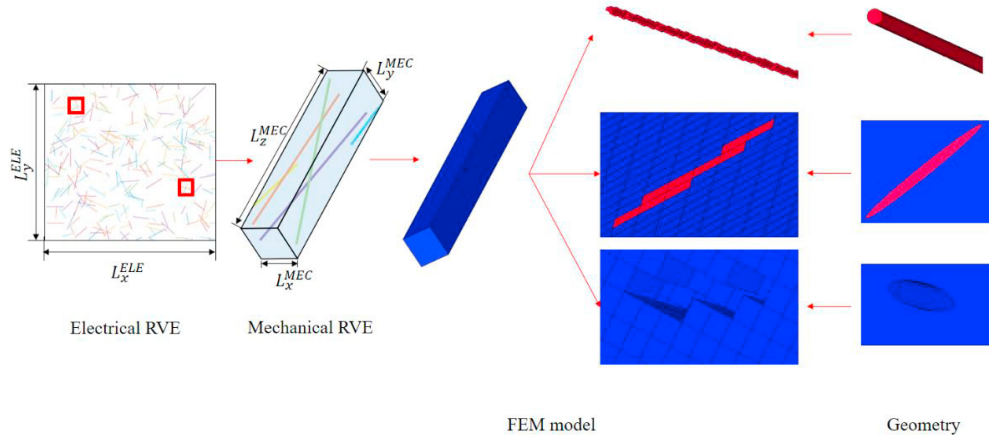

Fig. 5 Process of building the mechanical RVE FEM model

2.3 Coupled electromechanical model

Apart from mechanical properties evaluation, the change of electrical conductivity during the deformation of the nanocomposite i.e. piezoresistivity was also calculated. To this aim, the selection of the mechanical RVE models should include the effective current path. Note the change in resistance which is caused by other CNTs out of mechanical RVE models has been ignored, as no effective current path is generated among them. During the loading, the position of CNTs inside the mechanical RVE models were recorded. Subsequently, the resistance in every time step was calculated though the present electrical model. Therefore, the change of resistance due to the deformation of the CNT is also considered in this model.

3. Experiments

3.1 Material and preparation

In present study, Multi-Walled Carbon Nanotubes (purity > 99 wt.% and functional content 3.96 wt.%) were used, while the matrix was based on Araldite LY556 with a XB3473 hardener. Falling the addition of CNTs to the epoxy resin, a three-roller calendaring mill was used to evenly distribute CNTs. Finally, the harder was added to the epoxy resin at a volume ratio of 23:100 and the mixed resin was cured for 40min in air and 8h in vacuum in a vacuum bag at a temperature of 140˚C.

3.2 Tensile tests

Tensile tests were conducted according to the ASTM D638 standard with dimension shown in Fig.6. During the tensile test, the resistance change as a function of the strain increase throughout the gage length was recorded (Fig. 6). More details about tensile test setup and electromechanical characterizations can be found in (Esmaeili, Ma, et al. 2020; Esmaeili, Sbarufatti, et al. 2020).

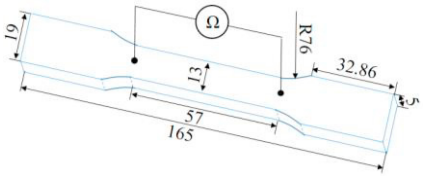

Fig. 6 Sample designed for tensile test

4. Results and discussion

4.1 Initial electrical property

In this section, the electrical model mentioned above was used to study the effect of the maximum polar angle θ_{max} on the electrical conductivity of the nanocomposites. Nanocomposites with 0.5 wt.% were considered to assess the current numerical method. The relative properties are shown in Table 1 and Table 2. The size of the electrical RVE should be set slightly larger than the length of CNT in order to get a stable result and high computational efficiency. Therefore, the lateral size of the electrical RVE cube is 5 μm.

Table 1. properties of the MWCNT used in the present study

Parameter	Description	Value
ρ_{MWCNT} /$g \cdot cm^{-3}$	Density	2.6
σ_{CNT} /$S \cdot m^{-1}$	Electrical conductivity	5000
ΔE /eV	Height of barrier	1
$\acute{l}$ /nm	Average length of CNT	5000
D /nm	Diameter of CNT	13.5
M	Number of tunneling channels	450
d_{vdW} / Å	Van der Waals separation distance	3.4
d_{cutoff} /nm	Cut-off distance in the tunneling effect	1.4
E /GPa	Elastic modulus	2000

Table 2. Properties of the epoxy used in the present study

Parameter	Description	Value
ρ_{epoxy} /$g \cdot cm^{-3}$	Density	1.14
σ_{epoxy} /$S \cdot m^{-1}$	Electrical conductivity	~10^{-11}
E /GPa	Elastic modulus	3.0
μ	Poisson's ratio	0.3

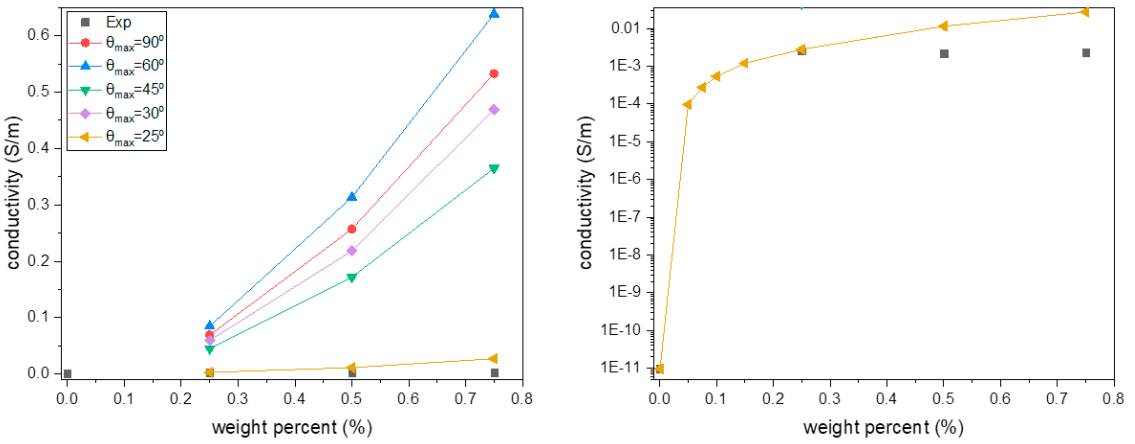

(a) (b)

Fig. 7 Comparison of the electric conductivity between numerical results and experimental data (a); agreement on electrical conductivity between simulated and experimental results (b)

In Fig. 7a, the results from the electrical model are compared with experimental data at different weight concentrations so that the maximum polar angle fitted in the present study can be defined for modelling. It implies that the best fitted results emerged when $\theta_{max} = 25°$, as visible in Fig. 7b. The results with the maximum polar angle 25° for more types of weight percentage were obtained through a numerical calculation. Additionally, nanocomposites with the higher the percentage of the weight percentage can cause more agglomeration and the higher number of defects. As a result, the error between the experimental and numerical data increased with the increase of the weight percentage. However, the results of 0.5 wt.% on the conductivity are still acceptable, which indicates that the further studies can be conducted in this direction.

4.2 Mechanical property

In the present study, the mechanical properties of MWCNT and epoxy are reported in Table 1 and Table 2. Perfect elastic was used to describe the behaviours of MWCNTs, while MAT_024 was applied on the matrix. The plasticity of the matrix was defined by the input data from the tensile tests, as presented in works about related epoxy resin (Ma et al. 2020; Esmaeili, Ma, et al. 2020). The uniaxial tensile tests conducted on the neat epoxy was the same as the present experimental activities. The size of the mechanical RVEs was 0.63×0.61×5.5 μm containing 1280000 elements. In addition, CONSTRAINED was employed as the boundary condition to keep the deformation on the same surface equal in order to replicate the uniform stress state (Ma et al. 2019; Ma, Giglio, and Manes 2020b). Regarding the interface property between the CNT and matrix, the strength of the interface along the normal direction was regarded as perfect bonding, while the shear strength was 36 MPa (Alian, Kundalwal, and Meguid 2015).

Fig. 8 shows the constitutional curves of 0.5 wt.% nanocomposite under different uniaxial loading directions. The differences in the mechanical property between x and y directions are negligible. The mechanical behaviours along both axials share the same Young's modulus, while the strength varies by 0.4%. On the contrary, the strength along z-direction is higher than in the other two directions (Fig. 8b), which indicates that this direction should be the enhanced orientation of the nanocomposite. Similar results were also shown in (Frankland et al. 2003). Moreover, the load is difficult to distribute along the transverse direction using a small polar angle, and therefore the strength is approximately equal to the failure strength of the interface. Thus, material can be strengthened along the direction of the CNT. The comparison between the numerical and experimental data is also shown in Fig. 8a, it can be observed that simulated results from loading along the x-/y-directions match experimental data leading to the validation of the current numerical model.

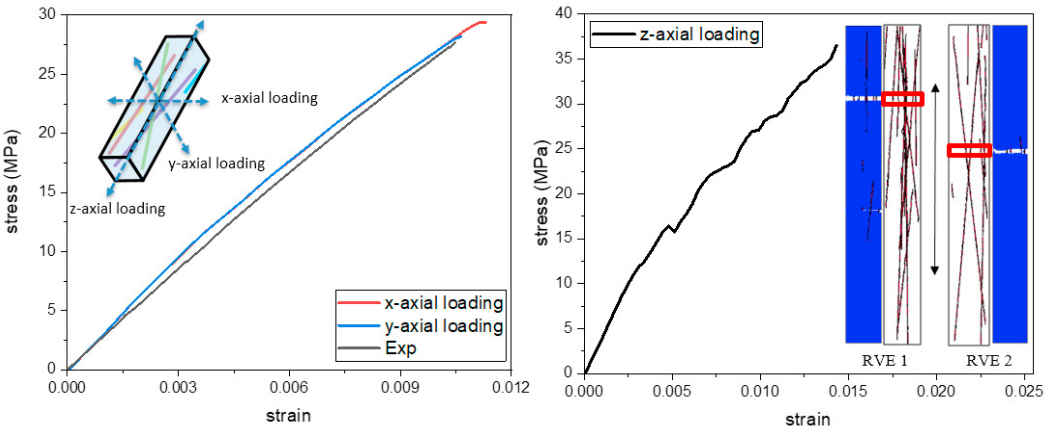

Fig. 8 Stress-strain curves under different uniaxial loading directions: (a) x- and y-axial loading; (b) z-axial loading

4.3 Change of conductivity during loading

By updating the distance matrix in each time step during loading process, the normalized resistance change can

be obtained as presented in Fig. 9 manifesting an increase in response of strain during tensile loading. Although noise was present during the recording in the experimental activities, the experimental and numerical results have good agreement with each other according to Fig. 9. The accurate replication of the electrical properties during loading with the current multi-physics method provides possibilities for monitoring mechanical behaviours of the nanocomposite using piezoresistive properties.

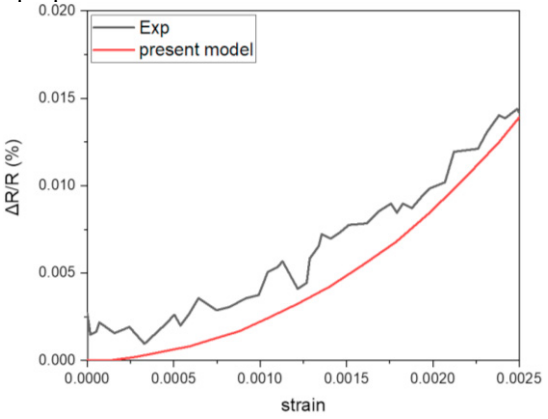

Fig. 9 Comparison of the resistance change during deformation between experimental and numerical results

5. Conclusion

With the introduction of an effective CNT to simplify the modelling process of the actual CNT, a multi-physics numerical method containing the mechanical and electrical models was proposed to mimic the mechanical behaviours of nanocomposite according to the initial electrical conductivity. The stress-strain obtained from the numerical model matched the experimental data, validating the current modelling strategy. Furthermore, the normalized resistance change with respect to the strain during tensile loading was also replicated through the current method, providing the possibility for the health monitoring of nanocomposite. The main conclusions drawn are listed below:

- The model generated from the electrical conductivity can be used to analyse the mechanical properties through a validation with the experimental data.
- The current numerical model can help to characterize the CNT networks inside the polymer, and to further investigate the mechanical and electrical behaviours of nanocomposites.
- The resistance change during deformation was predicted by the present methodology.

References

Alian, A. R., S. El-Borgi, and S. A. Meguid. 2016. “Multiscale Modeling of the Effect of Waviness and Agglomeration of CNTs on the Elastic Properties of Nanocomposites.” *Computational Materials Science* 117: 195–204. https://doi.org/10.1016/j.commatsci.2016.01.029.

Alian, A. R., and S. A. Meguid. 2017. “Molecular Dynamics Simulations of the Effect of Waviness and Agglomeration of CNTs on Interface Strength of Thermoset Nanocomposites.” *Physical Chemistry Chemical Physics* 19 (6): 4426–34. https://doi.org/10.1039/c6cp07464b.

Alian, A.R., S.I. Kundalwal, and S.A. Meguid. 2015. “Interfacial and Mechanical Properties of Epoxy Nanocomposites Using Different Multiscale Modeling Schemes.” *Composite Structures* 131 (November): 545–55. https://doi.org/10.1016/J.COMPSTRUCT.2015.06.014.

Alian, A.R., and S.A. Meguid. 2018a. “Large-Scale Atomistic Simulations of CNT-Reinforced Thermoplastic Polymers.” *Composite Structures* 191 (May): 221–30. https://doi.org/10.1016/J.COMPSTRUCT.2018.02.056.

Alian, A R, and S A Meguid. 2018b. “Multiscale Modeling of the Coupled Electromechanical Behavior of Multifunctional Nanocomposites.” *Composite Structures* 208 (October 2018): 826–35. https://doi.org/https://doi.org/10.1016/j.compstruct.2018.10.066.

———. 2018c. “Hybrid Molecular Dynamics--Finite Element Simulations of the Elastic Behavior of Polycrystalline Graphene.” *International Journal of Mechanics and Materials in Design* 14 (4): 551–63. https://doi.org/10.1007/s10999-017-9389-y.

Bao, W. S., S. A. Meguid, Z. H. Zhu, and M. J. Meguid. 2011. “Modeling Electrical Conductivities of Nanocomposites with Aligned Carbon Nanotubes.” *Nanotechnology* 22 (48). https://doi.org/10.1088/0957-4484/22/48/485704.

Bao, W.S., S.A. Meguid, Z.H. Zhu, Y. Pan, and G.J. Weng. 2012. “A Novel Approach to Predict the Electrical Conductivity of Multifunctional Nanocomposites.” *Mechanics of Materials* 46 (March): 129–38. https://doi.org/10.1016/J.MECHMAT.2011.12.006.

Bao, W S, S A Meguid, Z H Zhu, Y Pan, and G J Weng. 2013. “Effect of Carbon Nanotube Geometry upon Tunneling Assisted Electrical

Network in Nanocomposites." *Journal of Applied Physics* 113 (23). https://doi.org/10.1063/1.4809767.
Büttiker, M, Y Imry, R Landauer, and S Pinhas. 1985. "Generalized Many-Channel Conductance Formula with Application to Small Rings." *Phys. Rev. B* 31 (10): 6207–15. https://doi.org/10.1103/PhysRevB.31.6207.
Chen, X., A.R. Alian, and S.A. Meguid. 2019. "Modeling of CNT-Reinforced Nanocomposite with Complex Morphologies Using Modified Embedded Finite Element Technique." *Composite Structures* 227 (November): 111329. https://doi.org/10.1016/J.COMPSTRUCT.2019.111329.
Chen, X.L., and Y.J. Liu. 2004. "Square Representative Volume Elements for Evaluating the Effective Material Properties of Carbon Nanotube-Based Composites." *Computational Materials Science* 29 (1): 1–11. https://doi.org/10.1016/S0927-0256(03)00090-9.
Coleman, J N, S Curran, A B Dalton, A P Davey, B Mccarthy, W Blau, and R C Barklie. 1998. "Percolation-Dominated Conductivity in a Conjugated-Polymer-Carbon-Nanotube Composite" 58 (12): 7492–95. https://doi.org/10.1103/PhysRevB.58.R7492.
Danikas, Michael G. n.d. "Nanocomposites — A Review of Electrical Treeing and Breakdown," 19–25.
Eberly, David H. 2001. "3D Game Engine Design." *Kaufmann, San Francisco*.
Esmaeili, A., D. Ma, A. Manes, T. Oggioni, A. Jiménez-Suárez, A. Ureña, A.M.S. Hamouda, and C. Sbarufatti. 2020. "An Experimental and Numerical Investigation of Highly Strong and Tough Epoxy Based Nanocomposite by Addition of MWCNTs: Tensile and Mode I Fracture Tests." *Composite Structures* 252 (November): 112692. https://doi.org/10.1016/j.compstruct.2020.112692.
Esmaeili, A., C. Sbarufatti, D. Ma, A. Manes, A. Jiménez-Suárez, A. Ureña, D. Dellasega, and A.M.S. Hamouda. 2020. "Strain and Crack Growth Sensing Capability of SWCNT Reinforced Epoxy in Tensile and Mode I Fracture Tests." *Composites Science and Technology* 186 (January): 107918. https://doi.org/10.1016/j.compscitech.2019.107918.
Frankland, S.J.V., V.M. Harik, G.M. Odegard, D.W. Brenner, and T.S. Gates. 2003. "The Stress–Strain Behavior of Polymer–Nanotube Composites from Molecular Dynamics Simulation." *Composites Science and Technology* 63 (11): 1655–61. https://doi.org/10.1016/S0266-3538(03)00059-9.
Hertel, Tobias, Robert E Walkup, and Phaedon Avouris. 1998. "Deformation of Carbon Nanotubes by Surface van Der Waals Forces." *Phys. Rev. B* 58 (20): 13870–73. https://doi.org/10.1103/PhysRevB.58.13870.
Hu, Ning, Yoshifumi Karube, Cheng Yan, Zen Masuda, and Hisao Fukunaga. 2008. "Tunneling Effect in a Polymer/Carbon Nanotube Nanocomposite Strain Sensor." *Acta Materialia* 56 (13): 2929–36. https://doi.org/10.1016/j.actamat.2008.02.030.
Khan, Shafi Ullah, Jayaram R. Pothnis, and Jang-Kyo Kim. 2013. "Effects of Carbon Nanotube Alignment on Electrical and Mechanical Properties of Epoxy Nanocomposites." *Composites Part A: Applied Science and Manufacturing* 49 (June): 26–34. https://doi.org/10.1016/J.COMPOSITESA.2013.01.015.
Khattab, I.Al., and M. Sinapius. 2019. "Multiscale Modelling and Simulation of Polymer Nanocomposites Using Transformation Field Analysis (TFA)." *Composite Structures* 209 (February): 981–91. https://doi.org/10.1016/J.COMPSTRUCT.2018.10.100.
Li, Chunyu, Erik T. Thostenson, and Tsu Wei Chou. 2007. "Dominant Role of Tunneling Resistance in the Electrical Conductivity of Carbon Nanotube-Based Composites." *Applied Physics Letters* 91 (22). https://doi.org/10.1063/1.2819690.
Liu, Y.J, and X.L Chen. 2003. "Evaluations of the Effective Material Properties of Carbon Nanotube-Based Composites Using a Nanoscale Representative Volume Element." *Mechanics of Materials* 35 (1–2): 69–81. https://doi.org/10.1016/S0167-6636(02)00200-4.
Ma, Dayou, Ali Esmaeili, Andrea Manes, Claudio Sbarufatti, Alberto Jiménez-Suárez, Marco Giglio, and Abdel Magid Hamouda. 2020. "Numerical Study of Static and Dynamic Fracture Behaviours of Neat Epoxy Resin." *Mechanics of Materials* 140 (January): 103214. https://doi.org/10.1016/J.MECHMAT.2019.103214.
Ma, Dayou, Marco Giglio, and Andrea Manes. 2020a. "Analysis of Mesoscale Modelling Strategies for Woven Composites." *Material Design & Processing Communications*, no. January (February): mdp2.145. https://doi.org/10.1002/mdp2.145.
———. 2020b. "An Investigation into Mechanical Properties of the Nanocomposite with Aligned CNT by Means of Electrical Conductivity." *Composites Science and Technology* 188 (March): 107993. https://doi.org/10.1016/J.COMPSCITECH.2020.107993.
Ma, Dayou, Álvaro González-Jiménez, Marco Giglio, Christian Matheus dos Santos Cougo, Sandro Campos Amico, and Andrea Manes. 2021. "Multiscale Modelling Approach for Simulating Low Velocity Impact Tests of Aramid-Epoxy Composite with Nanofillers." *European Journal of Mechanics - A/Solids*, April, 104286. https://doi.org/10.1016/j.euromechsol.2021.104286.
Ma, Dayou, Andrea Manes, Sandro Campos Amico, and Marco Giglio. 2019. "Ballistic Strain-Rate-Dependent Material Modelling of Glass-Fibre Woven Composite Based on the Prediction of a Meso-Heterogeneous Approach." *Composite Structures* 216 (May): 187–200. https://doi.org/10.1016/j.compstruct.2019.02.102.
Ma, Dayou, Andrea Manes, and Marco Giglio. 2019. "The Effect of Mesh Morphologies on the Mesoscale Finite Element Modelling of Woven Composites." *Procedia Structural Integrity* 24 (January): 80–90. https://doi.org/10.1016/J.PROSTR.2020.02.007.
Sánchez-Romate, Xoan F., Joaquín Artigas, Alberto Jiménez-Suárez, María Sánchez, Alfredo Güemes, and Alejandro Ureña. 2018. "Critical Parameters of Carbon Nanotube Reinforced Composites for Structural Health Monitoring Applications: Empirical Results versus Theoretical Predictions." *Composites Science and Technology*, December. https://doi.org/10.1016/J.COMPSCITECH.2018.12.010.
Shams, Shahrooz, and Behzad Soltani. 2017. "The Effects of Carbon Nanotube Waviness and Aspect Ratio on the Buckling Behavior of Functionally Graded Nanocomposite Plates Using a Meshfree Method." *Polymer Composites* 38: E531–41. https://doi.org/10.1002/pc.23814.
Simmons, John G. 1963. "Generalized Formula for the Electric Tunnel Effect between Similar Electrodes Separated by a Thin Insulating Film." *Journal of Applied Physics* 34 (6): 1793–1803. https://doi.org/10.1063/1.1702682.
Wang, Shiren, Zhiyong Liang, Ben Wang, and Chuck Zhang. 2006. "Statistical Characterization of Single-Wall Carbon Nanotube Length Distribution." https://doi.org/10.1088/0957-4484/17/3/003.
Zabihi, Zabiholah, and Houshang Araghi. 2016. "Monte Carlo Simulations of Effective Electrical Conductivity of Graphene / Poly (Methyl Methacrylate) Nanocomposite : Landauer-Buttiker Approach." *Synthetic Metals* 217: 87–93. https://doi.org/10.1016/j.synthmet.2016.03.024.